Science Advances

AAAS

advances.sciencemag.org/cgi/content/full/2/4/e1501489/DC1

Supplementary Materials for

A broadband chip-scale optical frequency synthesizer at 2.7×10^{-16} relative uncertainty

Shu-Wei Huang, Jinghui Yang, Mingbin Yu, Bart H. McGuyer, Dim-Lee Kwong, Tanya Zelevinsky, Chee Wei Wong

Published 22 April 2016, *Sci. Adv.* **2**, e1501489 (2016)
DOI: 10.1126/sciadv.1501489

The PDF file includes:

I. Properties of the Si_3N_4 microresonator

Figure S1A shows a cross-section scanning electron micrograph of the microresonator waveguide, with an estimated 82° to 88° slope of the vertical sidewalls. The refractive index of the low pressure chemical vapor deposition (LPCVD) Si_3N_4 film was measured with an ellipsometric spectroscopy (Woollam M-2000 ellipsometer) and then fitted with the Sellmeier equation assuming a single absorption resonance in the ultraviolet. The fitted Sellmeier equation, $n(\lambda) = \sqrt{1 + \frac{2.90665\lambda^2}{\lambda^2 - 145.05007^2}}$, and the sidewall angle were both imported into the COMSOL Multiphysics for the microresonator design. Figure S1B shows the modeled free spectral range (FSR) of the first two TE modes of the microresonator. While the fundamental mode features a FSR of 17.9 GHz, the TE_2 mode has a slightly lower FSR and thus the resonances of the TE_2 family approaches that of the fundamental family about every 4 nm ($\frac{FSR^2}{\Delta FSR} = 460GHz$). The mode interaction when the resonances are close leads to local disruption of the phase matching condition *(37-39)* and results in the periodic amplitude modulation on the Kerr comb spectrum (Fig. 1B).

Figures S1C and S1D show the modeled group velocity dispersion (β_2, GVD) and third order dispersion (β_3, TOD). The non-equidistance of the cold cavity modes, $D = (\omega_{m+1} - \omega_m) - (\omega_m - \omega_{m-1})$, can be calculated using the equation $D = -\frac{(\beta_2 L)}{2\pi}\omega_{FSR}^3 + \frac{(\beta_2 L)^2}{4\pi^2}\omega_{FSR}^5 - \frac{(\beta_3 L)}{4\pi}\omega_{FSR}^4$, where L is the cavity's length and ω_{FSR} is the cavity's free spectral range.

Due to the large refractive index of the Si_3N_4 waveguide, a 600 μm long adiabatic mode converter (the Si_3N_4 waveguide, embedded in the 5×5 μm^2 SiO_2 waveguide, has gradually changing widths from 0.2 μm to 1 μm) is implemented to improve the coupling efficiency from the free space to the bus waveguide. The input-output insertion loss for the waveguide does not exceed 6 dB.

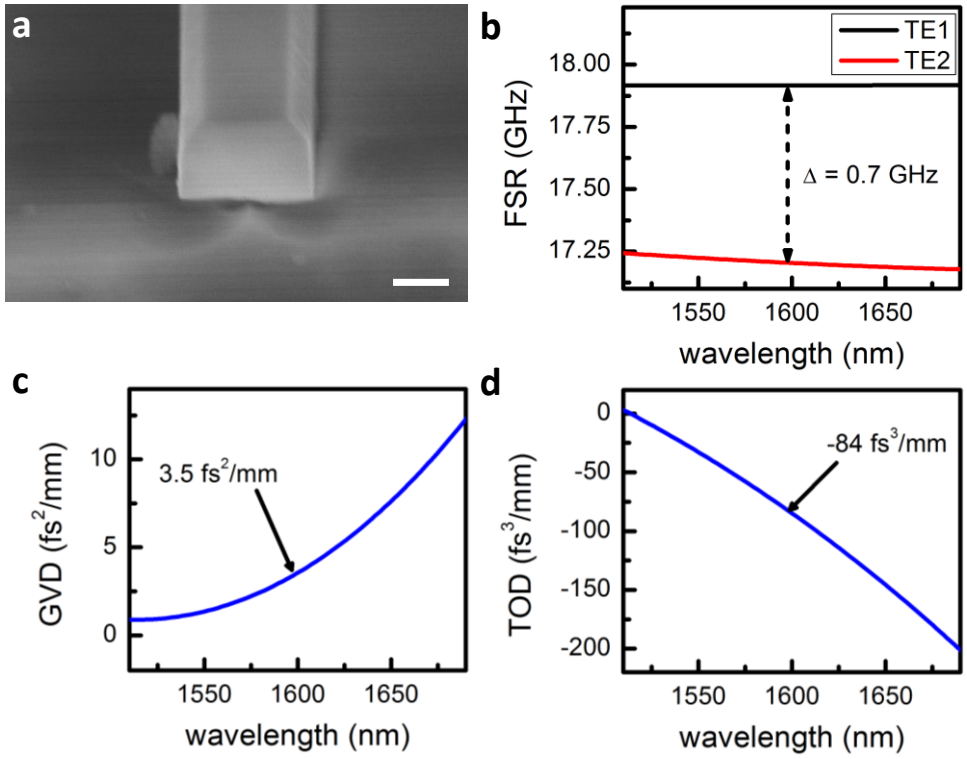

fig. S1. Properties of the Si_3N_4 microresonator. (a) Scanning electron micrograph of the waveguide cross-section. Scale bar: 500 nm. **(b)** Modeled free spectral range of the first two TE modes of the chip-scale optical frequency comb. **(c)** Modeled group velocity dispersion of the fundamental mode, measuring a GVD of 3.5 fs^2/mm at the pump wavelength. **(d)** Modeled third order dispersion of the fundamental mode, measuring a TOD of -84 fs^2/mm at the pump wavelength.

II. Low-noise state of the Kerr frequency comb

As the pump wavelength was tuned into the resonance from the high frequency side, we first observed multiple RF spikes because the primary comb line spacing is incommensurate with the fundamental comb spacing. The state with incommensurate spacing was unstable and it made frequent transition to high-noise state characterized by elevated RF amplitude noise (45 dB higher than the phase-locked comb state). Next, with fine control of the pump wavelength (10 MHz/step), the offset between different comb families can be made zero such that the RF amplitude noise spectrum showed no excess noise (fig. S2). The phase-locked comb typically stabilized for hours.

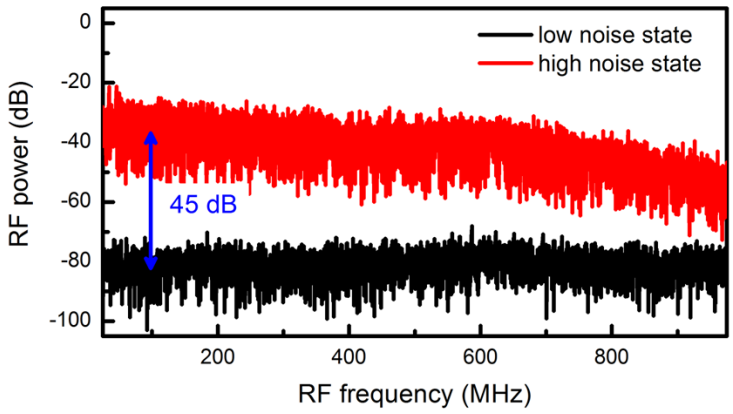

fig. S2. RF amplitude noise spectra of the high-noise state and the low-noise phase-locked comb state. With the proper pump wavelength, RF amplitude noise dropped by 45 dB and approached the detector background noise, indicative of the transition into a phase-locked state.

III. Confirmation of continuously equidistant Kerr frequency comb

To verify the Kerr frequency comb is continuously equidistant, not consisted of many sub-comb families with offsets *(30)*, we measured the comb spacing and the amplitude noise of various different filtered segments of the Kerr frequency comb (1553.5-1554.5nm, 1555-1556nm, 1556.2-1557.2nm, 1558-1559nm, 1560-1561nm, 1561.7-1562.7nm, 1563.5-1564.5nm, 1566-1567nm, 1568.5-1569.5nm, 1570.5-1571.5nm, 1572.3-1573.3nm, 1574-1575nm, 1577-1578nm 1578.5-1579.5nm, 1580.3-1581.3nm). The comb spacing was measured to be identical at 17.9 GHz within the RBW of 390 kHz (fig. S3A) and 1 kHz (fig. S3B) for the 15 filtered comb segments from 1553.5nm to 1581.3nm. No other peaks were observed. Absence of sub-comb families with offset frequencies was also independently confirmed by the amplitude noise measurements, showing no peaks and excess noise above the detector background noise. The Kerr microcomb's continuous equidistance was thus verified.

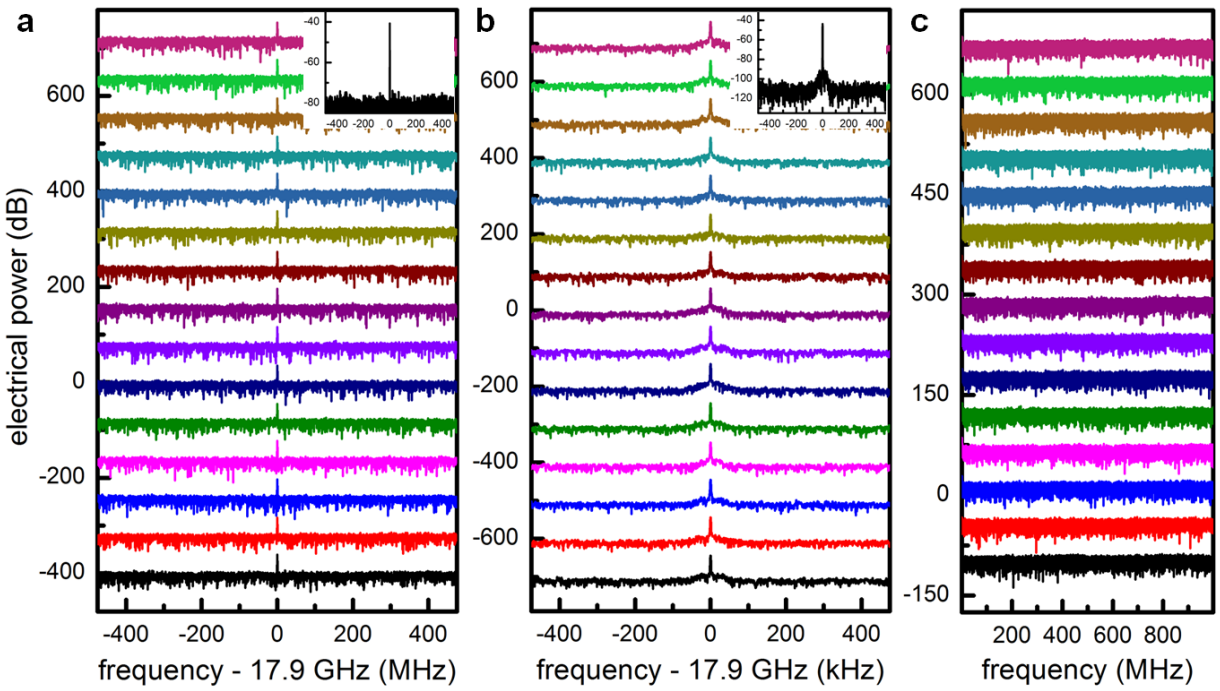

fig. S3. Confirmation of the continuously equidistant Kerr frequency comb. (a) Comb spacing spectra of 15 filtered comb segments with scan ranges of 1 GHz. **(b)** Comb spacing spectra of 15 filtered comb segments with scan ranges of 1 MHz. **(c)** Amplitude noise spectra of 15 filtered comb segments with a scan range of 1 GHz.

IV. Dependence of comb spacing on pump properties

After the Kerr frequency comb was driven into the low phase noise state, we characterized the dependence of the comb spacing on the pump properties by adding a 0.1 Hz sinusoidal change of either pump frequency or pump power and measuring the corresponding comb spacing oscillation amplitude with a frequency counter.

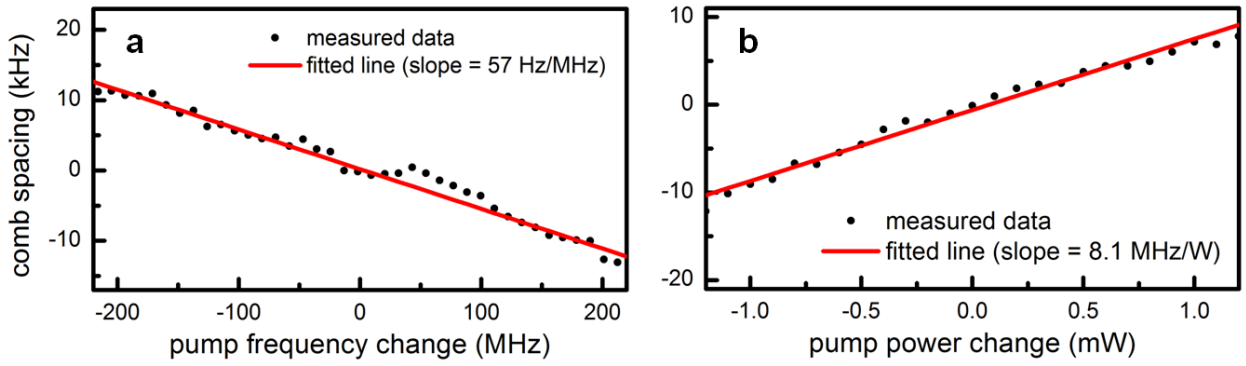

fig. S4. Dependence of comb spacing on pump properties. (a) The comb spacing as a function of the pump frequency change, determined at 57 Hz/MHz in our microresonator. **(b)** The comb spacing as a function of the pump power change in the ring, determined at 8.1 MHz/W in our microresonator.

V. After-resonator feedback stabilization scheme and measurements

As discussed in the main text, a rubidium locked diode laser at 1560 nm can also be used as the optical reference for phase locking one of the comb lines (*16, 33, 40*). As Si_3N_4 microresonators suffer from lower *Q* at optical C-band due to residual N-H absorption *(9)*, we prefer to pump the microresonator at optical L-band for low threshold comb generation. In the alternative scheme, the 1560 nm comb line is thus only accessible after the microresonator when the Kerr microcomb is generated (fig. S5). Here the 1560 nm comb line was selected by a narrowband monochromator and beat with the optical reference on a photodetector after the comb generation stage. The rest of the setup was the same as the one shown in Fig. 1A. Figure S5B shows that the beat note can be equally well stabilized to a resolution limited linewidth of 6 Hz.

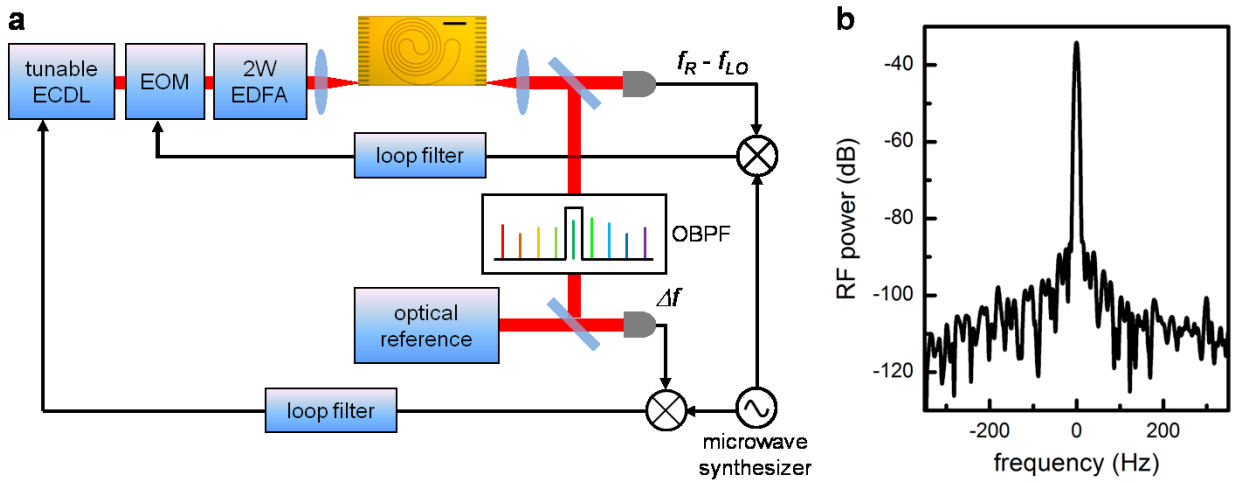

fig. S5. Schematic of the alternative experimental setup for the generation and stabilization of the chip-scale optical frequency comb. (a) After the microresonator, the 1560 nm comb line was selected by a narrowband monochromator and beat with the optical reference on a photodetector. The rest of the setup was the same as the one shown in Fig. 1A. **(b)** RF spectrum of the stabilized beat note, showing a resolution limited linewidth of 6 Hz. Control of the comb line frequency was achieved by modulating the diode current of the ECDL. OBPF: optical bandpass filter.